Dynamic Sensor Allocation Framework for Fault Tolerant Flight Control [★]

Tamás Péni [∗,∗∗] Bálint Vanek [∗] Zoltán Szabó [∗] József Bokor [∗]

[∗] *Institute for Computer Science and Control,*
Hungarian Academy of Sciences (MTA SZTAKI)
[∗∗] *corresponding author, (e-mail: pt@scl.sztaki.hu)*

Abstract: This paper proposes a novel method for sensor allocation based fault tolerant control. Fault tolerance is achieved with optimal combination of healthy sensor sources while the baseline controller remains unchanged. The measurements are subjected to various sensor dynamics, hence the resulting sensor allocation framework is also dynamic. The proposed approach can fit into a hierarchical fault tolerant control framework, where certain sensor faults are handled by the lower level allocation while more severe faults are handled by controller reconfiguration. The decision of which reconfiguration level has to be initiated in response to a fault is determined by a supervisor unit. The method is demonstrated on the simulation model of the Nasa AirStar test vehicle.

1. INTRODUCTION

A major trend in modern flight control system research for both manned and unmanned vehicles is the need to pursue improved reliability and environmental sustainability of safety critical systems Vanek et al. [2013], Goupil and Marcos [2012]. Faults and failures often result in loss of performance and may even in catastrophic harm or loss of life. For that reason, improving the safety and reliability of civil aircraft via improving the pilots or operators abilities to counteract the faults and provide them the same handling qualities as long as possible are important priorities. Reconfigurable control methods are one way to compensate for failures or damage of flight control system-Ganguli et al. [2002], Steinberg [2005], but in most cases reconfiguration itself is a challenging task since it might introduce transients and providing bumpless transfer is non trivial when complex systems are under investigation. On the other hand, when the system has high amount of redundancy, which is often the case in aircraft, the actuators or sensors can be allocated without changing the baseline control system Enns [1998], Harkegard [2004] . This can be partially resolved by designing the control system to provide desired forces and moments, often the case in nonlinear dynamic inversion based control Directorate [1996], which is later transformed by a suitable control allocation method to surface deflections Johansen and Fossen. [2013]. It is also possible to adaptively estimate the control effectiveness and use that with the control distributor concept to allocate the available control effort Lombaerts et al. [2012] compensated with pseudo control hedging to handle unachievable commands. It is also possible to treat the actuator faults by dynamic allocation Zaccarian [2009], as well. Compared to the static allocation schemes, with dynamic allocators it is possible to eliminate the transients on the actuators caused by the configuration change.

Most reconfiguration methods are developed to handle actuator dynamics and very limited effort can be found in the literature to handle the sensor fault problem. Most of them are devoted to the virtual sensor approach Richter et al. [2011], where estimation based methods are used to replace the faulty measurement with its estimate. In other approaches estimate of the magnitude of sensor fault is used by the control scheme to accommodate faults by setpoint alteration Bonivento et al. [2003]. In Wu et al. [2006] sensor fault masking is used as a mean of FTC while redundancy is measured using the control reconfigurability proposed in Wu [2004]. More recently actuator and sensor faults are accommodated by parameter depending control scheme, where the controller is parameterized with the sensor fault magnitude in Cai and Wu [2010].

Commercial passenger jets have triple redundant sensor systems and so the likelihood of a catastrophic failure is extremely small but in very unlikely cases common mode failures have caused accidents in the past. The loss of the B-2 bomber in Guam is an interesting case where moisture in the Air Data System caused the miscalibration of several Port Transducer Units. This initiated a tightly coupled chain of events that culminated in the B-2s crash. Similar accidents have been reported where bird strike caused loss of pitot probes, considered also a common mode failure. While these accidents are very unlikely some form of contingency plan against them can further increase the level of aviation safety, by providing improved functionality for the pilot under failure operation. This might include the preserving of pilot aids like flight envelope protection instead of present day practice reverting to the direct law.

The aim of the paper is to present a dynamic sensor allocation based fault tolerant control strategy for commercial aircraft. The baseline control system is designed for the nominal dynamics of the aircraft with redundancy in the sensor measurements, while in the event of faults the sensor reallocation scheme is able to accommodate additional sensor measurements, subjected to different sensor characteristics in a dynamic manner. The proposed approach assumes a fault detection and isolation (FDI) algorithm running on-board the aircraft, which is able to identify the fault in time. FDI methods developed especially to detect aircraft sensor failures can be found e.g. in Berdjaga et al. [2012], van Eykeren and Chu [2013], van Eykeren et al. [2012], Alwi and Edwards [2011]. The design of the proposed reconfigurable control algorithm is based on Linear Time Invariant (LTI) systems but its extension to Linear Parameter-varying (LPV) control methods seems feasible to handle larger flight envelopes.

Also the nullspace based methods in Varga [2009], used in the calculation of allocation strategy, have many similarities with the geometric methods of Balas et al. [2003] applied to LPV systems. The prime advantage of this approach is that baseline multivariable controller with stability and robustness guarantees remains unchanged during reconfiguration. The design is demonstrated on the simplified simulator model of the NASA AirSTAR Flight Test Vehicle. The paper is organized as follows. Section 3 presents the proposed sensor reallocation procedure. In Section 4 and Section 5 introduce the model of the NASA AIRStar UAV and synthesis of the baseline controller. The simulation results are collected in Section 6. Conclusions are drawn in Section 7.

2. NOTATION

The notation used in the paper are fairly standard. The transfer function of a linear, time invariant system $\dot{x} = Ax + Bu$, $y = Cx + Du$ is denoted by $G(s) = \left[\begin{array}{c|c} A & B \\ \hline C & D \end{array}\right] = C(sI - A)^{-1}B + D$. If M is a constant or a transfer function matrix then we refer to its (i,j)-th element, its i-th row and its jth column as $M_{i,j}$, $M_{i,*}$ and $M_{*,j}$, respectively. For a given $G(s)$, we will denote by $G_\perp(s)$ the left annihilator of $G(s)$, which is a stable transfer function satisfying $G_\perp(s)G(s) = 0$. Clearly, $G_\perp(s)$ lies in the (left) nullspace of the rational matrix $G(s)$. The basis of the nullspace and a particular $G_\perp(s)$ itself can be efficiently determined from the state-space representation of $G(s)$ by using either the matrix pencil algorithms documented in Varga [2008, 2009] or the routines implemented in the Linear Fractional Representation (LFR) Toolbox Magni [2004, 2006]. (In this paper, we used the latter, i.e. the dynamical kernels were computed by the `null` function of the LFR Toolbox.)

3. SENSOR REALLOCATION

We assume that the system to be controlled is linear, time-invariant given by its transfer-function $P(s)$. The input to the plant is denoted by u and the measured output is denoted by y. The latter is assumed to be partitioned into y_K and y_R, i.e. $y = \left[\begin{array}{c} y_K \\ y_R \end{array}\right]$. They are assumed to be measured via the known, linear, time-invariant sensor dynamics $S_K(s) \in \mathcal{RH}_\infty$ and $S_R(s) \in \mathcal{RH}_\infty$, respectively. Let $S_A(s)$ be the LTI dynamics of the actuators and suppose that a baseline controller $K(s)$ has already been designed for the augmented system

$$\bar{P}(s) = S_K(s)P(s)S_A(s) \qquad (1)$$

such that the closed loop dynamics satisfies all prescribed stability and performance requirements. It can be seen from (1) that the controller is designed to use only the y_K measurements. The remaining outputs y_R provide extra-measurements that can be used to substitute a faulty sensor in $S_K(s)$. In order that the components of y_K can be reproduced from the elements of y_R we will assume that the following relation holds between the two vectors:

$$y_R = Uy_K$$

where U is a known matrix of suitable dimension. If $S_K(s)y_K$ and $S_R(s)y_R$ are denoted by y_K^m and y_R^m and $S_K(s)$ has a stable inverse, then the measurement equation can be formulated as

$$y^m = \left[\begin{array}{c} y_K^m \\ y_R^m \end{array}\right] = \left[\begin{array}{c} I \\ S_R(s)US_K(s)^{-1} \end{array}\right] S_K(s)y_K$$

Remark 1. If $S_K(s)$ is not stably invertible (e.g. because it contains strictly proper transfer functions and/or has

right half-plane zeros) then it can be still enough to be 'approximately' invertible, i.e. there exists $S_K^\dagger(s) \in \mathcal{RH}_\infty$ s.t. $S_K^\dagger(s)S_K(s) = Z(s)$ satisfies $Z(0) = I$, $Z(s) \in \mathcal{RH}_\infty$ and the poles of $Z(s)$ are larger than the bandwidth of the controller. Moreover, by designing the controller to be suitably robust, the perturbation caused by the approximate inversion can be further attenuated.

During normal operation, when all sensors in $S_K(s)$ are healthy, this measurement vector is projected onto the input of $K(s)$ via the trivial projection $V = [I\ 0]$, $(y_K^m = Vy^m)$. The aim of the forthcoming sensor reallocation procedure is to provide efficient fault accommodation without modifying the baseline controller. For this, the sensor reconfiguration has to be totally unseen by the controller. This can be achieved if V is replaced by $V + \bar{E}(s)$, where $\bar{E}(s)$ is chosen such that

$$\bar{E}(s) \left[\begin{array}{c} I \\ S_R(s)US_K(s)^{-1} \end{array}\right] = 0. \qquad (2)$$

Introducing $M(s) = I$ and $N(s) = S_R(s)US_K(s)^{-1}$ the column matrix $\left[\begin{array}{c} M(s) \\ N(s) \end{array}\right]$ can be considered as a right co-prime factorization of $G(s) = N(s)M(s)^{-1} = N(s) = S_R(s)US_K(s)^{-1}$. From the properties of coprime factorization it follows that there exist transfer functions $\tilde{N}(s), \tilde{M}(s) \in \mathcal{RH}_\infty$ such that

$$\left[\begin{array}{cc} -\tilde{N}(s) & \tilde{M}(s) \end{array}\right] \left[\begin{array}{c} M(s) \\ N(s) \end{array}\right] = 0. \qquad (3)$$

One possible realization of these transfer functions can be obtained if $G(s) = \left[\begin{array}{c|c} A & B \\ \hline C & D \end{array}\right]$ is observable and L is an arbitrary observer gain rendering $A + LC$ stable:

$$\left[\begin{array}{cc} -\tilde{N}(s) & \tilde{M}(s) \end{array}\right] = \left[\begin{array}{c|cc} A+LC & -(B+LD) & H \\ \hline C & -D & I \end{array}\right] \qquad (4)$$

Due to (3) we can choose $E(s) = \left[\begin{array}{cc} -\tilde{N}(s) & \tilde{M}(s) \end{array}\right]$ and $\bar{E}(s) = R(s)E(s)$, where $R(s) \in \mathcal{RH}_\infty$ is an arbitrary transfer function.

In case of sensor faults one or more sensors measuring y_K, become useless and - depending on the fault (runaway, jamming, etc.) - start producing wrong measurements. If there is a fault detection and isolation filter implemented in the control loop, then the faulty sensors can be efficiently identified. Having determined the location of the faults, the reconfiguration mechanism has to substitute the faulty sensors by using the measurement redundancy provided by y_R^m. The straightforward way to perform this task is to select $R(s)$ so that $V + \bar{E}(s) = V + R(s)E(s)$ realizes 0 transfer from the faulty sensors. If doing so, the faulty measurements cannot deteriorate the control performance and, due to (2), the controller will not see anything from this configuration-change.

To explain the mechanism of the sensor allocator design, assume that the i-th and the j-th sensors are faulty. Their effect is exactly separated from the control loop if the i-th and j-th columns of $V + \bar{E}(s) = V + R(s)E(s)$ are 0, i.e. $R(s)$ is chosen so that

$$\left[\begin{array}{cc} \bar{E}_{*,i}(s) & \bar{E}_{*,j}(s) \end{array}\right] = -\left[\begin{array}{cc} V_{*,i} & V_{*,j} \end{array}\right].$$

Since V consists of an identity and a zero matrix the rows of $R(s)$ can be determined by using system inversion and nullspace computation routines. In our particular case
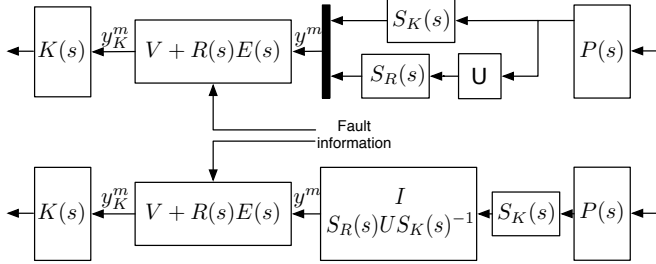
Fig. 1. Reconfiguration scheme: implementation (top) and design (bottom) forms. The implementation form illustrates the structure of how the sensor reallocation is implemented in the control loop. The design form is equivalent to the implementation form, but it is used to construct the reallocation filter $V + R(s)E(s)$.

$$\begin{bmatrix} V_{*,i} & V_{*,j} \end{bmatrix} = \begin{bmatrix} 0 & 0 \\ .. & .. \\ 1 & 0 \\ .. & .. \\ 0 & 1 \\ .. & .. \end{bmatrix} \begin{matrix} .. \\ .. \\ \rightarrow i \\ \\ \rightarrow j \\ \end{matrix}, \quad \text{if } i < j.$$

So let Q (or $Q(s)$) be an arbitrary (transfer function-) matrix, which renders

$$\begin{bmatrix} E_{*,i} & E_{*,j} & Q \end{bmatrix}$$

invertible. If the inverse is denoted by $W(s)$ then we can choose $R_{i,*}(s) = -W_{1,*}(s)$ and $R_{j,*}(s) = -W_{2,*}(s)$. The remaining rows of $R(s)$ can be freely selected from the rows of $[E_{*,i}(s) \ E_{*,j}(s)]_\perp$.

To apply this reconfiguration method in practice, a set of $R(s)$ filters have to be designed – one for each possible fault scenario. These filters are then stored on the on-board computer and in case of a fault the filter corresponding to the detected fault combination is activated.

4. BASELINE CONTROL DESIGN MODEL

An effective resource for experimentally testing flight control algorithms, including adaptive control algorithms, is the Airborne Subscale Transport Aircraft Research (AirSTAR) testbed at NASA Langley Research Center Murch [2008]. The primary AirSTAR flight test vehicle is a turbine powered 5.5% dynamically scaled model of a civilian transport aircraft, often referred to as the Generic Transport Model (GTM). The GTM has a wing span of $7ft$, and weighs around $55lbs$. Under normal operations, it flies at an altitude of 700 to $1100ft$, with an airspeed between 70 and 85 knots. The currently used T-2 test aircraft is shown in Fig. 2. Significant wind tunnel and flight testing has been performed to identify the flight dynamics of the GTM Cunningham et al. [2008]. A nonlinear simulation model of the aircraft dynamics has been developed and is readily available to the research community. Experimental control algorithms are easily embedded in this simulation model for verification prior to flight testing Dorobantu et al. [2012]. Hence, the AirSTAR testbed is a highly effective for experimental flight control research through its flexible architecture and rapid implementation and testing cycle. GTM nonlinear simulation model is trimmed to steady level flight at 60 knots and linearized to obtain a linear model of the aircraft dynamics. A twelve state, full-order linear model is generated for the given flight condition. The longitudinal model includes five states: u forward velocity, w normal velocity, q pitch rate, h altitude, and θ pitch angle. In addition to full state measurement, air data sensors measure V_{cas} calibrated airspeed, and angle-of-attack α. The inertial measurement

Fig. 2. The NASA AIRStar vehicle.

unit also provides forward (a_x) and normal acceleration (a_z). Hence a total of 9 measurements are available for longitudinal control purposes.

The control inputs to the model are left and right inner and outer elevator deflections $\delta_{e,LI}$, $\delta_{e,LO}$, $\delta_{e,RI}$, $\delta_{e,RO}$ $[rad]$, 4 spoiler deflections $\delta_{sp_{1,2,3,4}}[rad]$, 4 flap deflections $\delta_{fl_{1,2,3,4}}[rad]$, and left and right throttle $\delta_{THR,L}, \delta_{THR,R}[\%]$. The longitudinal LTI state-space model of the GTM is given in the form of:

$$\begin{bmatrix} \dot{u} \\ \dot{w} \\ \dot{q} \\ \dot{h} \\ \dot{\theta} \end{bmatrix} = A_{lon} \begin{bmatrix} u \\ w \\ q \\ h \\ \theta \end{bmatrix} + B_{lon} \begin{bmatrix} \delta_e \\ \delta_{sp} \\ \delta_{fl} \\ \delta_{THR} \end{bmatrix} \quad (5)$$

where the control inputs are grouped to simplify the controller design, at the expense of loosing input redundancy. The outputs are the five states and the four additional measured signals from air data and inertial measurements.

$$\begin{bmatrix} u \\ w \\ q \\ h \\ \theta \\ V_{cas} \\ \alpha \\ a_x \\ a_z \end{bmatrix} = \begin{bmatrix} I_{5 \times 5} \\ C_{V,\alpha,a_x,a_z} \end{bmatrix} \begin{bmatrix} u \\ w \\ q \\ h \\ \theta \end{bmatrix} + \begin{bmatrix} 0_{7 \times 4} \\ D_{a_x,a_z} \end{bmatrix} \begin{bmatrix} \delta_e \\ \delta_{sp} \\ \delta_{fl} \\ \delta_{THR} \end{bmatrix} \quad (6)$$

The plant is augmented with first order actuator dynamics of $G_{act} = \frac{2\pi 5}{s+2\pi 5}$ on elevator, spoiler and flaps and $G_{eng} = \frac{-0.1474s+0.7314}{s^2+1.336s+0.7314}$ on the the throttle, which contains a right half plane zero, which are all passed through via a 4th order Pade approximation filter representing the $0.03\ s$ delay associated with sampling and computational time. Sensor dynamics are omitted in the original GTM model, but for the research purpose the current investigation includes sensor dynamics from Fielding et al. [2002]. The following sensor models are used for inertial measurements, air data sensors and Euler angle estimates respectively: $S_{in} = \frac{0.0001903s^2+0.005346s+1}{0.0004942s^2+0.03082s+1}$; $S_{air} = \frac{1}{0.02s+1}$; $S_{Ea} = \frac{1}{0.00104s^2+0.0323s+1}$. The resulting system with delay, sensor and actuator dynamics has 39 states.

5. LONGITUDINAL CONTROL DESIGN

The baseline controller for pitch angle (θ) tracking and velocity set point following is designed for the LTI model of the GTM at 60 knots using $\mathcal{H}_\infty$ synthesis technique with measurements of $V_{cas}, \alpha, q, h, \theta$, the remaining measurements of u, a_x, a_z are used as redundant measurements utilised during the sensor allocation. The system interconnection (Fig. 3) addressing the tracking problem assuming model mismatches and exogenous disturbance is detailed in the following. The influence of actuator
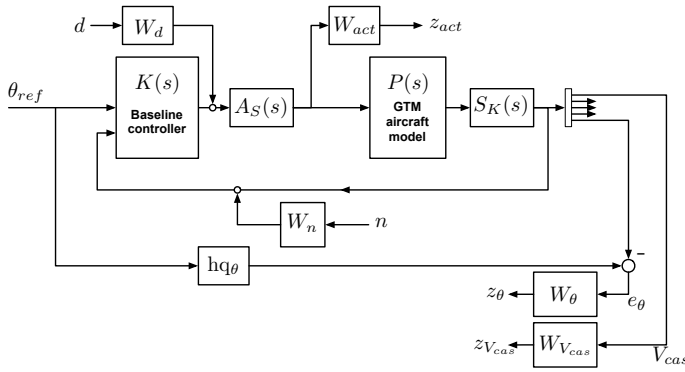
Fig. 3. Block diagram for baseline controller synthesis.

input uncertainty is denoted with W_d with weight of $W_d = \text{diag}(0.5I_{3\times 3}; 10)$ with lower uncertainty on elevator, spoiler and flap, while higher uncertainty on the throttle channel, mainly due to the slower dynamics and discontinuous nature of the throttle logic.

Actuator usage is penalised in the design with weights of $W_{act} = \text{diag}(1/5, 1/0.1, 1/0.5, 1/5)$ corresponding to the allowed magnitude of deflection in the robust control synthesis, where elevator usage is preferred over spoiler and flap deflections, while engine inputs are also having higher weights with respect to their range of $[0 - 100]\%$.

Characteristics of the noise is captured by $W_n = \text{diag}(0.25; 0.15; 0.2; 0.25; 0.05)$ with higher amount of noise on air data related quantities and lower noise on inertial quantities.

Model matching is achieved by filtering the reference signal through a "handling-qualities" model (hq_θ) to achieve smooth behavior with adequate speed of response for pitch angle commands. The model represents the ideal behavior of the vehicle for pilot inputs, it has adequate speed of response with respect to the short period dynamics $hq_\theta = \frac{2^2}{s^2+4s+2^2}$.

The main control objective, to keep the error between the plant output θ and the desired response hq_θ low, is weighted across frequency with $W_\theta = 25\frac{1^2}{s^2+2s+1^2}$ across all parameter range, trading off good steady state tracking with degraded performance at frequencies higher than $5\ rad/s$. An additional control requirement is to keep V_{cas} low in the LTI design, meaning following the trim set points on velocity. This objective has lower relative importance and since the velocity dynamics is significantly slower its weight is more important below $0.01\ rad/s$, hence $W_{V_{cas}} = 0.1\frac{0.025^2}{s^2+0.05s+0.025^2}$.

The weights are optimised to have the best tradeoff between good command tracking and disturbance rejection. Having performed the $\mathcal{H}_\infty$ synthesis we achieved $\gamma = 1.5963$ for the upper bound of the $\mathcal{H}_\infty$-norm measured between $w_p = [d, n, \theta_{ref}]$ and $z_p = [z_{act}, z_\theta, z_{V_{cas}}]$. (The controller was designed by using the Robust Control Toolbox of MATLAB.)

6. SIMULATION RESULTS

As stated above the measurements of $V_{cas}, \alpha, q, h, \theta$ are used in the baseline control design, but air data sensors can be affected by common mode failures such as bird strike or miscalibration due to probe heating or icing. Hence the remaining measurements of u, w, a_x, a_z can be used as

backup solution. In order to apply the method proposed in Section 3, first the control-input dependence of a_x and a_z has to be compensated by using the control input and the sensor dynamics. Then the computations can be continued with $\hat{a}_x$ and $\hat{a}_z$, the dynamics of which do not contain direct feedthrough terms. Let $y_K = [V_{cad}, \alpha, q, h, \theta]$ and $y_R = [u, w, \hat{a}_x, \hat{a}_z]$. Between these two vectors the following relation holds:

$y_R = Uy_K$, where

$$U = \begin{bmatrix} 0.9896 & -0.2572 & 0 & 0 & 0 \\ 0.1438 & 1.7697 & 0 & 0 & 0 \\ 0.0272 & 0.5084 & -0.2292 & -0.0002 & -0.5557 \\ -0.6193 & -3.6227 & 1.6240 & 0.0009 & -0.0808 \end{bmatrix}$$

The sensor dynamics corresponding to y_K and y_R are as follows:

$$S_K(s) = \text{diag}(S_{air}(s), S_{air}(s), S_{in}(s), S_{air}(s), S_{Ea}(s))$$
$$S_R(s) = \text{diag}(S_{air}(s), S_{air}(s), S_{in}(s), S_{in}(s))$$
$$S_{air}(s) = \frac{1}{0.02s+1},$$
$$S_{in}(s) = \frac{0.0001903s^2 + 0.005346s + 1}{0.0004942s^2 + 0.03082s + 1},$$
$$S_{Ea}(s) = \frac{1}{0.00104s^2 + 0.0323s + 1}$$

Since $S_K(s)$ contains strictly proper transfer functions, it is not invertible. Therefore, an approximate inverse has been constructed by completing the improper inverses with additional, suitably large stable poles:

$$S_K^\dagger(s) = \text{diag}(S_{air}^\dagger(s), S_{air}^\dagger(s), S_{in}^{-1}(s), S_{air}^\dagger(s), S_{Ea}\dagger(s))$$
$$S_{air}^\dagger(s) = \frac{2s+100}{s+100},$$
$$S_{in}^{-1}(s) = \frac{0.0004942s^2 + 0.03082s + 1}{0.0001903s^2 + 0.005346s + 1},$$
$$S_{Ea}^\dagger(s) = \frac{0.00104s^2 + 0.0323s + 1}{6.667e - 06s^2 + 0.005333s + 1}$$

Having constructed the (approximate) inverses we computed $E(s)$ from the state space realisation of $G(s) = S_R(s)US_K^\dagger(s)$ by using formula (4). The observer gain required to determine the coprime factors was chosen to be the optimal LQ control gain computed for the pair (A^T, C^T) with wights $Q = I$ and $R = 0.1I$. Then $R(s)$ was constructed according to the procedure described in Section 3.

In the simulation the fault occurred at $t = 4s$. The detection time was $0.15s$, that is the reconfiguration of the sensors was initiated only at $t = 4.15s$. (We assume that the sensor loss does not cause such large transients during this short time period, which cannot be attenuated if the reconfiguration is switched on.)

The figures below present the results of three simulation runs: the first is the nominal case, when no sensor fault occurred. In the second case the effect of the simultaneous failure of the V_{cas} and q sensors were simulated and no sensor reconfiguration was used. The failure we emulated was a runaway fault, when the output of the sensor was drifting from the nominal value by means of a ramp function of slope 2. The third simulation presents the case, when the proposed fault accommodation procedure was active. The results of the simulations are depicted in Figs. 4-5-6. It can be seen that the failure of the 2 sensors resulted in the loss of stability (Fig. 5). Fig. 6 certifies that the stability (together with the nominal
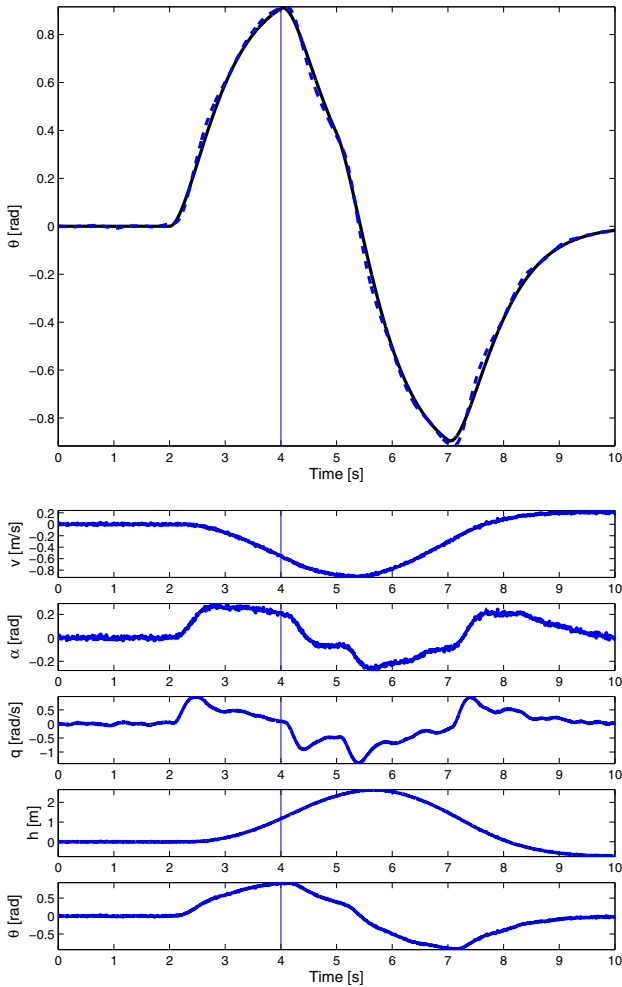
Fig. 4. Normal operation (without fault) with baseline controller. Tracking of θ-reference (top) and (sensory) inputs to the controller (bottom). In the top figure the continuous curve represents the θ-reference (a doublet filtered via $hq_\theta(s)$), while the dashed curve is the output of the GTM model.

Fig. 5. Simultaneous runaway fault on V_{cas} and q sensors without reallocation. Tracking of θ-reference (top) and inputs to the controller (bottom). Due to the fault, the first and the third sensors started drifting from the true value. The effect of the fault can be seen in the top figure: the stability was lost.

control performance) could be successfully regained if sensor reallocation was applied. It can also be seen that the reallocation procedure ensured that the controller got (after a short transient) almost the same sensory information than in the nominal case. This means that the fault remained totally hidden from the controller and thus had no effect on the control performance.

7. CONCLUSION

A novel sensor reconfiguration procedure has been proposed in the paper. The method is based on redundant sensor measurements and provides efficient fault accommodation without modifying the baseline controller. The heart of the algorithm is the construction of a dynamic left nullspace of a specific LTI generated by the augmented sensor dynamics. Although there are infinitely many transfer functions describing the same nullspace, in this paper we have not exploited this freedom yet. We have chosen only one arbitrary annihilator, focusing only on its stability. Continuing this research, the proposed design can be further improved by choosing the annihilator dynamics more carefully, so that other design specifications (e.g. robustness against modelling uncertainties, sensitivity to

external disturbances) can also be taken into consideration. Moreover, the LFT representation makes it possible to extend our approach to parameter-varying systems as well.

REFERENCES

H. Alwi and C. Edwards. Evaluation of sliding mode observers for fault reconstruction on the ADDSAFE functional engineering simulator. *SAE Int. J. Aerosp*, 4(2):1485–1499, 2011.

G. Balas, J. Bokor, and Z. Szabo. Invariant subspaces for LPV systems and their applications. *IEEE Transactions on Automatic Control*, 48(11):2065–2069, 2003.

D. Berdjaga, J. Cieslakb, and A. Zolghadri. Fault diagnosis and monitoring of oscillatory failure case in aircraft inertial system. *Control Engineering Practice*, 20(12): 1410–1425, 2012.
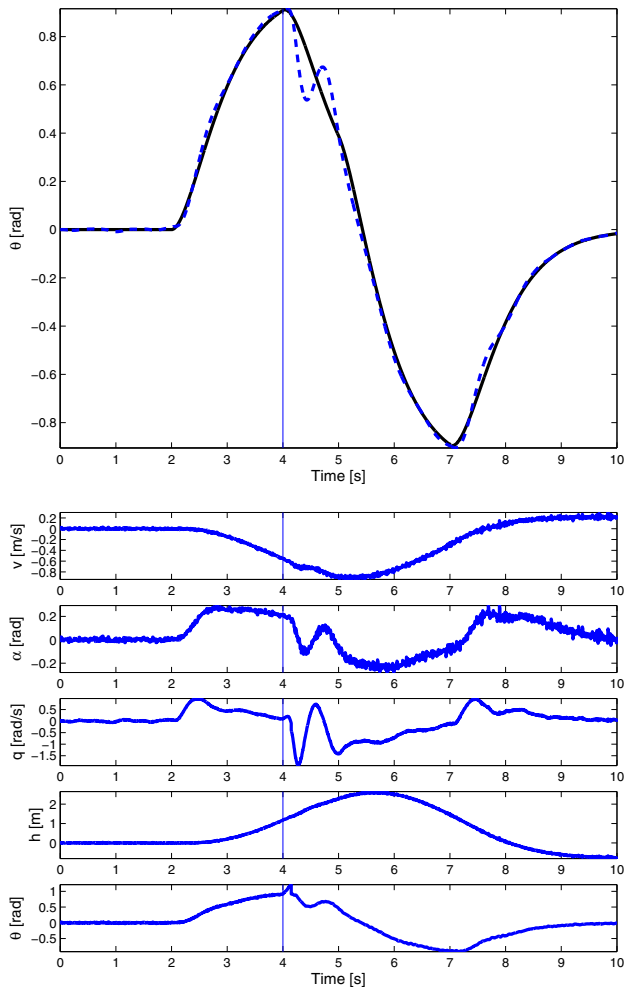
Fig. 6. Simultaneous runaway fault on V_{cas} and q sensors with sensor reallocation. Tracking of θ-reference (top) and inputs to the controller (bottom). Although 2 of the 5 sensors were useless, the reallocation assured that the controller got almost the same sensory information than in the nominal case. This means that the fault remained totally hidden from the controller and thus had no (harmful) effect on the control performance.

C. Bonivento, A. Paoli, and L. Marconi. Fault-tolerant control of the ship propulsion system benchmark. *Control Engineering Practice*, 11(5):483–492, 2003.

X. Cai and F. Wu. Robust parameter-dependent fault tolerant control for actuator and sensor faults. *International Journal of Control*, 83(7):1475–1484, 2010.

K. Cunningham, J. V. Foster, A. M. Murch, and E. Morelli. Practical application of a subscale transport aircraft for flight research in control upset and failure conditions. In *AIAA Guidance, Navigation, and Control Conference*, 2008.

Flight Dynamics Directorate. Application of multivariable control theory to aircraft control laws. Technical report, Honeywell TC and Lockheed Martin, 1996.

A. Dorobantu, A. M. Murch, and G. J. Balas. h_∞ robust control design for the nasa airstar flight test vehicle. In *50th AIAA Aerospace Sciences Meeting*, 2012.

D. F. Enns. Control allocation approaches. In *AIAA Guidance, Navigation, and Control Conference*, 1998.

C. Fielding, A. Varga, S. Bennani, and M. Selier, editors. *Advanced Techniques for Clearance of Flight Control Laws*. Springer-Verlag, 2002.

S. Ganguli, A. Marcos, and Gary Balas. Reconfigurable lpv control design for boeing 747-100/200 longitudinal axis. In *American Control Conference, 2002. Proceedings of the 2002*, volume 5, pages 3612–3617 vol.5, 2002. doi: 10.1109/ACC.2002.1024489.

Ph. Goupil and A. Marcos. Industrial benchmarking and evaluation of addsafe fdd designs. In *Fault Detection, Supervision and Safety of Technical Processes (8th SAFEPROCESS)*, 2012.

O. Harkegard. Dynamic control allocation using constrained quadratic programming. *Journal of Guidance, Control, and Dynamics*, 2004.

T. A. Johansen and T. I. Fossen. Control allocation - a survey. *Automatica*, 49(1087-1103), 2013.

T.J.J. Lombaerts, G.H.N. Looye, Q.P. Chu, and J.A. Mulder. Design and simulation of fault tolerant flight control based on physical approach. *Aerospace Science and Technology*, 23:151–171, 2012.

J.-F. Magni. Linear fractional representations with a toolbox: modelling order reduction, gain scheduling, version 1.1. Technical report, ONERA-CERT, Department of Systems Control and Flight Dynamics, Tolouse, France, 2004.

J.-F. Magni. User manual of the Linear Fractional Representation Toolbox. Technical report, ONERA-CERT, Department of Systems Control and Flight Dynamics, Tolouse, France, 2006.

A. M. Murch. A flight control system architecture for the nasa airstar flight test infrastructure. In *AIAA Guidance, Navigation, and Control Conference*, 2008.

J.H. Richter, W.P.M.H. Heemels, N. van de Wouw, and J. Lunze. Reconfigurable control of piecewise affine systems with actuator and sensor faults: Stability and tracking. *Automatica*, 47:678–691, 2011.

M. Steinberg. A historical overview of research in reconfigurable flight control. *Aerospace Control and Guidance Systems Committee Meeting No. 95*, Subcomitee E:1–38, 2005.

L. van Eykeren and Q. P. Chu. *Advances in Aerospace Guidance, Navigation and Control*, chapter Air Data Sensor Fault Detection Using Kinematic Relations, pages 183–197. Springer, 2013.

L. van Eykeren, Q. P. Chu, and J. A. Mulder. Sensor fault detection and isolation using adaptive extended kalman filter. In *8th IFAC Symposium on Fault Detection, Supervision and Safety of Technical Processes*, pages 1155–1160, 2012.

B. Vanek, T. Peni, Z. Szabo, P. Gaspar, and J. Bokor. Supervisory fault tolerant control of the GTM UAV using LPV methods. In *2nd International Conference on Control and Fault Tolerant Systems (Systol'13)*, Nice, 2013.

A. Varga. On computing nullspace bases - a fault detection perspective. In *17th IFAC World Congress*, pages 6295–6300, 2008.

A. Varga. The nullspace method-a unifying paradigm to fault detection. In *IEEE Conference on Decision and Control*, pages 6964–6969, 2009.

N. E. Wu. Coverage in fault-tolerant control. *Automatica*, 40(4):537–548, 2004.

N. E. Wu, S. Thavamania, Y. Zhang, and M. Blanke. Sensor fault masking of a ship propulsion system. *Control Engineering Practice*, 14:1337–1345, 2006.

L. Zaccarian. Dynamic allocation for input redundant control systems. *Automatica*, 45:1431–1438, 2009.